Closed-Form CRLBs for SNR Estimation from Turbo-Coded Square-QAM-Modulated Signals

Faouzi Bellili, Achref Methenni, and Sofiène Affes
INRS-EMT, 800, de la Gauchetière Ouest, Bureau 6900, Montreal, Qc, H5A 1K6, Canada.
Emails: {bellili,methenni,affes}@emt.inrs.ca,

***Abstract*—In this contribution, we derive for the first time the closed-form expressions for the Cramér-Rao lower bounds (CRLBs) of the signal-to-noise ratio (SNR) estimates from turbo-coded square-QAM transmissions. By exploiting the structure of the Gray mapping, we are able to factorize the likelihood function thereby linearizing all the derivation steps for the FIM elements. The analytical CRLBs coincide exactly with their empirical counterparts validating thereby our new analytical expressions. Numerical results suggest that the CLRBs for code-aided (CA) SNR estimates range between the CRLBs for non-data-aided (NDA) SNR estimates and those for data-aided (DA) ones, thereby highlighting the effect of the coding gain. At sufficiently high SNR levels, the three CRLBs coincide. The derived bounds are also valid for LDPC-coded systems and they can be evaluated in the same way when the latter are decoded using the turbo principal.**

***Index Terms*—Signal-to-noise ratio (SNR), Cramér-Rao lower bound (CRLB), Turbo/LDPC codes, Extrinsic information, Gray mapping, Square QAMs.**

I. Introduction

In modern wireless communication systems, the SNR is considered as a key parameter whose *a priori* knowledge (estimation) is required in multiple applications such as equalization [1, 2], adaptive modulation, link adaptation, and power control [3, 4], just to name a few. Depending on the *a priori* knowledge about the transmitted sequence, SNR estimators can be broadly divided into two major categories: i) data-aided (DA) techniques which base the estimation process on perfectly known (pilot) sequences, and ii) non-data-aided (NDA) techniques where the SNR is estimated blindly, i.e., with no available information about the transmitted symbols. Although NDA approaches do not impinge on the whole throughput of the system, they exhibit poor estimation performance at low SNRs and/or with short data records. In such harsh conditions, code-aided (CA) estimation can be envisaged to substantially enhance performance while being spectrally efficient.

Turbo codes [5] have gained considerable attention due to their impressive ability to operate in the near-Shannon limit even at very low SNRs. In order to satisfy the ever increasing demand in high data rates, the use of turbo codes in conjunction with high-order QAMs has been already adopted in many current and upcoming wireless communication standards such as 4G long-term evolution (LTE), LTE-advanced (LTE-A) and beyond (LTE-B) [6, 7].

Recently, it has been shown in (see [8-11] and references therein) that the SNR estimation performance can be substantially enhanced by exploiting some priors that are delivered during the decoding process of the transmitted bits. Indeed, over a wide range of practical SNRs, CA estimation was found to perform nearly the same as DA estimation. In turbo-coded systems, for instance, CA estimation schemes may rely on the *soft* information delivered by the soft-input soft-output (SISO) decoder.

The effect of the SNR mismatch on the performance of turbo-coded systems has been the subject of various studies. In the presence of higher-order-modulated signals, it was found [12] that the estimated SNR plays a different role in the calculation of the bit metric for each modulation scheme, thereby leading to different decoding performance. The performance of turbo-coded systems transmitting higher-order-modulated signals is typically more sensitive to SNR over-estimation [12].

Due to the emergence of various SNR-dependent adaptive signalling schemes, SNR estimation has recently witnessed a surge of interest with a main focus on diversity-reception systems. In fact, a bunch of advanced NDA SNR estimtors have been recently proposed in [13-17] for both *constant* and *time-varying* single-input multiple-output (SIMO) channels. SNR estimators suited for turbo-coded single-input single-output (SISO) systems have also been recently reported in the open literature (see [8-10] and references therein). The performance of such estimators is usually assessed in terms of error variance; yet it still requires to be gauged against an absolute benchmark that sets the minimum achievable variance for all the unbiased estimators. Unlike other loose bounds, the the *stochastic*[1] Cramér-Rao lower bound (CRLB) [18] is usually used as a benchmark since it can be achieved, asymptotically, by the stochastic maximum likelihood estimator. More than a decade ago, the *stochastic* CRLBs of NDA SNR estimates were derived in closed form [19] for the special cases of BPSK and QPSK signals only. It was only recently that their analytical expressions were developed for arbitrary higher-order square QAM modulations [20, 21]. In CA estimation, however, such *stochastic* CRLBs were derived analytically for the very basic case of coded BPSK transmissions only [11] and their closed-form expressions for higher-order modulations have not been reported yet. A compelling illustration of the literature limitation persisting so far is that code-aided SNR estimators have been very often compared in performance to the DA CRLBs (as recently done in [9] and [11]). The latter might offer an accurate benchmark for BPSK signals, but become excessively optimistic[2] in the presence of higher-order-modulated signals, especially at low SNR values (see section V for more details).

Motivated by all the aforementioned facts, we derive in this paper for the very first time the closed-form expressions of the CRLBs for CA SNR estimation from turbo-coded square-QAM-modulated signals. Numerical results will show that the new analytical CRLBs coincide with their empirical counterparts obtained by following the same approach of [22]. They will also reveal that the CA scheme lies between the NDA and DA schemes in terms of CRLB performance limit, acting therefore as its upper and lower ends, respectively. The CA's performance bound moves up or down to either ends with the coding rate relatively decreasing or increasing, respectively. Furthermore, all three CRLBs tend to coincide at higher SNR values.

The rest of this paper is structured as follows. In section II, we present the system model. In section III, we introduce the new recursive process that allows the construction of any square-QAM Gray-coded constellation and we relate the symbols' *a priori*

Work supported by the Discovery Grants Program of NSERC and a Discovery Accelerator Supplement (DAS) Award.

[1]The stochastic designation is usually adopted to refer to the case of unknown and random transmitted symbols. This is in contrast with the *deterministic* CRLB where the symbols are unknown but deterministic.

[2]The DA CRLBs are indeed the same for all linearly-modulated signals [19], i.e., they would misleadingly suggest the same bound regardless of the modulation type or order if taken as a benchmark when it is, in fact, different in CA transmissions.

978-1-4799-3512-3/14/$31.00 ©2014 Crown

probabilities to the bits' log-likelihood ratios (LLRs). In section IV, we factorize the probability density function (pdf) of each received sample into two analogous terms. In section V, we derive the different FIM elements and the analytical expressions for the considered CA CRLBs. In section VI, we present the simulation results of the newly derived bounds and, finally, draw out some concluding remarks in section VII.

In the following, vectors and matrices will be represented in lower- and upper-case bold fonts, respectively. Moreover, $\{.\}^T$ and $\{.\}^H$ will denote the transpose and the Hermitian (transpose conjugate) operators, respectively. The operators $\Re\{.\}$ and $\Im\{.\}$ will return, respectively, the real and imaginary parts of any complex number whereas $\{.\}^*$ and $|.|$ will return its conjugate and its amplitude, respectively. We will denote by j the pure complex number that verifies $j^2 = -1$ and $E\{.\}$ stands for statistical expectation. We will also denote the probability mass function (PMF) for discrete random variables by $Pr[.]$ and the probability density function (pdf) for continuous random variables by $p[.]$.

II. System Model

Consider a turbo-coded system where a binary sequence of information bits (grouped into consecutive blocks containing Q bits each) is fed into a turbo encoder, of rate R. The encoder consists of two identical recursive and systematic convolutional codes (RSCs) with generator polynomials $[g1,\ g2]$. The two RSCs are concatenated in parallel via an interleaver of size L. The coded bits are then fed into a puncturer which selects an appropriate combination of the parity bits, from both encoders, in order to achieve the desired overall rate R. Each block of Q coded bits (systematic and parity bits) is scrambled with an outer interleaver, and then mapped onto any Gray-coded square-QAM constellation. Finally, the obtained symbols are transmitted over the wireless channel and the received signal is sampled at the output of the matched filter. By assuming *imperfect* phase and frequency synchronization, the received samples are modeled for $k = 0, 1, 2, \cdots, K-1$ as follows:

$$y(k) \quad = \quad S\ x(k)e^{j2\pi k\vartheta+\phi} + w(k), \tag{1}$$

where, at time index k, $x(k)$ is the k^{th} coded transmitted symbol. The channel is assumed to be slowly time-varying, over the entire observation window of size K, and hence of constant but unknown gain, S, and phase shift ϕ. The parameter ϑ stands for the normalized carrier frequency offset (CFO). The noise components, $w(k)$, are modeled by zero-mean complex circular Gaussian random variables, with independent real and imaginary parts, each of variance σ^2 (i.e., of total noise power $N_0 = 2\sigma^2$). Without loss of generality, we further assume that the energy of the transmitted symbols is normalized to one, i.e., $\mathrm{E}\{|x(k)|^2\} = 1$. Using the multiple observations $\{y(k)\}_{k=0}^{K-1}$, the true SNR, ρ, to be estimated is defined as:

$$\rho \quad = \quad \frac{\mathrm{E}\{S^2|x(k)|^2\}}{2\sigma^2} = \frac{S^2}{2\sigma^2}. \tag{2}$$

For mathematical convenience, we define the parameter vector $\boldsymbol{\alpha} = [S \quad \sigma^2]$ and we gather all the received samples in a single vector $\boldsymbol{y} = [y(0), y(1), \cdots, y(K-1)]^T$. In addition, since using the decibels (dB) scale often provides easier interpretation of the performance behavior, we will henceforth consider the following parameter transformation:

$$g(\boldsymbol{\alpha}) = 10\log_{10}\left(S^2/2\sigma^2\right). \tag{3}$$

As shown in [18], the CRLB for the parameter transformation in (3) is given by:

$$\mathrm{CRLB}(\rho) = \frac{\partial g(\boldsymbol{\alpha})}{\partial \boldsymbol{\alpha}} \boldsymbol{I}^{-1}(\boldsymbol{\alpha}) \frac{\partial g(\boldsymbol{\alpha})}{\partial \boldsymbol{\alpha}}^T, \tag{4}$$

where $\boldsymbol{I}(\boldsymbol{\alpha})$ is the Fisher information matrix (FIM) whose entries are expressed as:

$$[\boldsymbol{I}(\boldsymbol{\alpha})]_{i,l} = -\mathrm{E}\left\{\frac{\partial^2 L_{\boldsymbol{y}}(\boldsymbol{\alpha})}{\partial\alpha_i\partial\alpha_l}\right\} \qquad i,l = 1,2. \tag{5}$$

In (5), $\{\alpha_i\}_{i=1,2}$ are the elements of the unknown parameter vector $\boldsymbol{\alpha}$ and $L_{\boldsymbol{y}}(\boldsymbol{\alpha}) = \ln\left(p[\boldsymbol{y};\boldsymbol{\alpha}]\right)$ is the log-likelihood function (LLF) of the system $\big(p[\boldsymbol{y};\boldsymbol{\alpha}]$ being the pdf of $\boldsymbol{y}$ parameterized by $\boldsymbol{\alpha}\big)$. As seen from (5), the first step in deriving the tackled bounds is to find an explicit expression for the LLF. To that end, the pdf $p[\boldsymbol{y};\boldsymbol{\alpha}]$ must established and thus the *a priori* probabilities, $Pr[x(k) = c_m]$, of the transmitted symbols involved in (1) must be found. In NDA estimation they are readily obtained as $Pr[x(k) = c_m] = 1/M$ for $m = 1, 2, \cdots, M$ since the transmitted symbols are usually assumed to be equally likely. In coded transmissions, however, the symbols are not equally likely and their *a priori* probabilities must be calculated. Indeed, in the next section, we will express them in terms of the LLRs of the conveyed bits. In practice, the information about the LLRs is acquired from the output of the SISO decoder at the convergence of the BCJR algorithm [24].

III. Derivation of the Symbols' *a priori* Probabilities

We assume the constellation to be Gray-coded and we denote its alphabet by $\mathcal{C}_p = \{c_0, c_1, \cdots, c_{M-1}\}$. Moreover, we will from now on adopt the two following notations:

$$c_m \longleftrightarrow \bar{b}_1^m \bar{b}_2^m \cdots \bar{b}_{\log_2(M)}^m, \qquad x(k) \longleftrightarrow b_1^k b_2^k \cdots b_{\log_2(M)}^k. \tag{6}$$

to designate the mapping between the m^{th} constellation point c_m $\big[$respectively, the k^{th} transmitted symbol $x(k)\big]$ and its associated Gray-coded bits $\big[$respectively, the k^{th} block of conveyed bits$\big]$. Due to the large-size interleaver, the coded bits can be assumed as statistically independent. This is a standard assumption in CA estimation practices $\big($see [22, 25, 26] and references therein$\big)$. Therefore, the *a priori* probability of each transmitted symbol factorizes into the elementary probabilities of its conveyed bits:

$$Pr[x(k) = c_m] = \prod_{l=1}^{\log_2(M)} Pr\left[b_l^k = \bar{b}_l^m\right]. \tag{7}$$

We also define the LLR of the l^{th} coded bit, b_l^k, conveyed by the symbol, $x(k)$, as follows:

$$L_l(k) \triangleq \ln\Big(Pr[b_l^k = 1]/Pr[b_l^k = 0]\Big). \tag{8}$$

Since $Pr[b_l^k = 0] + Pr[b_l^k = 1] = 1$, it can be shown that:

$$Pr[b_l^k = 1] = \frac{e^{L_l(k)}}{1 + e^{L_l(k)}} \quad \text{and} \quad Pr[b_l^k = 0] = \frac{1}{1 + e^{L_l(k)}}. \tag{9}$$

For every c_m in $\mathcal{C}_p$, if $x(k) = c_m$, the two identities in (9) can then be merged together to yield a generic expression:

$$Pr[b_l^k = \bar{b}_l^m] = \frac{1}{2\cosh\left(L_l(k)/2\right)} e^{(\bar{b}_l^m - 1)\frac{L_l(k)}{2}}, \tag{10}$$

in which $\bar{b}_l^m$ is either 0 or 1 depending on which of the symbols c_m is transmitted, at time instant k, and of course on the Gray mapping that is associated to the constellation in (6). Therefore, injecting (10) in (7) and recalling that square-QAM constellations verify $\log_2(M) = 2p$ for some integer $p \geq 2$, we obtain:

$$Pr[x(k) = c_m] = \underbrace{\left(\prod_{l=1}^{2p} \frac{1}{2\cosh\left(L_l(k)/2\right)}\right)}_{\beta_k} \prod_{l=1}^{2p} e^{(\bar{b}_l^m - 1)\frac{L_l(k)}{2}}. \tag{11}$$

Next, we describe a simple recursive process that allows the construction of arbitrary Gray-coded square-QAM constellations.

Owing to this recursive process, some hidden properties of such constellations will be revealed and carefully handled in order to rewrite the a priori probabilities in (11) in a more insightful form that will prove useful in the next section. In fact, using any *basic* Gray-coded QPSK and starting from any given $2^{2(p-1)}$-QAM Gray-coded constellation, it is possible to build another 2^{2p}-QAM Gray-coded one as follows:

- *step 1*: build the top-right quadrant of the desired 2^{2p}-QAM constellation from all the points of the available $2^{2(p-1)}$-QAM constellation. As such, all the points of the new quadrant are still missing 2 out of the $2p$ bits they must represent. This is simply because they were cloned from the given $2^{2(p-1)}$-QAM constellation whose points actually represent $2p-2$ bits only. For the sake of clarity and again w.l.o.g, we will assume that these two missing bits always occupy the two least significant positions in each point of the new quadrant.
- *step 2*: build the remaining empty quadrants (bottom-right, top-left and bottom-left) of the desired 2^{2p}-QAM constellation by symmetries with respect to the $x-$axis, the $y-$axis, and the center point, respectively. In light of "*step 1*", all the points of the desired constellation are inherently missing 2 bits each.
- *step 3*: copy the two bits of each quadrant in the basic Gray-coded QPSK constellation to all the points that belong to the same quadrant in the incomplete 2^{2p}-QAM constellation obtained in "*step 2*".

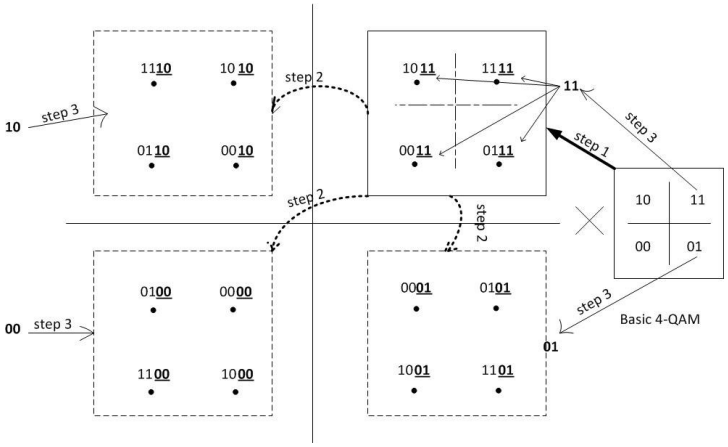

Fig. 1. Recursive construction of Gray-coded square-QAM constellations illustrated here from 4-QAM to 16-QAM.

One example that clearly depicts these three steps is shown in Fig. 1 (illustrated here in initial transition from 4-QAM to 16-QAM). It can be easily verified that this recursive process yields Gray-coded constellations.

Next, we further denote the top-right quadrant of the constellation by $\tilde{\mathcal{C}}_p$. As such, each point $c_m \in \mathcal{C}_p$ belongs to a set of four symmetrical points $\{\tilde{c}_m, \tilde{c}_m^*, -\tilde{c}_m, -\tilde{c}_m^*\}$ for some $\tilde{c}_m$ in $\tilde{\mathcal{C}}_p$. Moreover, due to symmetries of "*step 2*", these four symmetrical points share the same $2p-2$ most significant bits (MSBs), $\bar{b}_1^m \bar{b}_2^m \bar{b}_3^m ... \bar{b}_{2p-3}^m \bar{b}_{2p-2}^m$. Consequently, if we consider these $2(p-1)$ MSBs alone and we define the quantity:

$$\mu_{k,p}(c_m) \triangleq \prod_{l=1}^{2p-2} e^{(2\bar{b}_l^m - 1)\frac{L_l(k)}{2}}, \quad \forall\ c_m \in \mathcal{C}_p,\ p \geq 2, \tag{12}$$

it follows from (11) that:

$$Pr[x(k)=c_m] = \beta_k \mu_{k,p}(c_m) e^{(2\bar{b}_{2p-1}^m - 1)\frac{L_l(k)}{2}} e^{(2\bar{b}_{2p}^m - 1)\frac{L_l(k)}{2}}, \tag{13}$$

with:

$$\mu_{k,p}(\tilde{c}_m) = \mu_{k,p}(-\tilde{c}_m) = \mu_{k,p}(\tilde{c}_m^*) = \mu_{k,p}(-\tilde{c}_m^*). \tag{14}$$

From the right-hand side of (12), it is seen that $\mu_{k,p}(c_m)$ is not defined for $p=1$, i.e., for QPSK constellations. We extend its definition for the latter simply by taking $\mu_{k,1}(c_m) = 1\ \ \forall\ c_m \in \mathcal{C}_1$. It will be seen later that this choice is consistent with all the derivations.

Now, the two bits $\bar{b}_{2p-1}^m \bar{b}_{2p}^m$ involved in the two remaining exponentials in (13) are exactly the same for all the symbols that belong to the same quadrant in the obtained 2^{2p}-QAM constellation (recall that they are added in "*step 3*"). Typically, by considering the *basic* QPSK depicted in Fig. 1, they are given by "$\bar{b}_{2p-1}^m \bar{b}_{2p}^m$" = "11", "00", "01", and "10", for each $\tilde{c}_m \in \tilde{\mathcal{C}}_p$, $-\tilde{\mathcal{C}}_p$, $\tilde{\mathcal{C}}_p^*$, and $-\tilde{\mathcal{C}}_p^*$, respectively. By using these results in (13) and recalling (14), it follows that:

$$Pr[x(k)=\tilde{c}_m] = \beta_k\ \mu_{k,p}(\tilde{c}_m)\ e^{\frac{L_{2p-1}(k)}{2}} e^{\frac{L_{2p}(k)}{2}}, \tag{15}$$

$$Pr[x(k)=\tilde{c}_m^*] = \beta_k\ \mu_{k,p}(\tilde{c}_m)\ e^{-\frac{L_{2p-1}(k)}{2}} e^{\frac{L_{2p}(k)}{2}}, \tag{16}$$

$$Pr[x(k)=-\tilde{c}_m] = \beta_k\ \mu_{k,p}(\tilde{c}_m)\ e^{-\frac{L_{2p-1}(k)}{2}} e^{-\frac{L_{2p}(k)}{2}}, \tag{17}$$

$$Pr[x(k)=-\tilde{c}_m^*] = \beta_k\ \mu_{k,p}(\tilde{c}_m)\ e^{\frac{L_{2p-1}(k)}{2}} e^{-\frac{L_{2p}(k)}{2}}. \tag{18}$$

IV. Derivation of the LLF for Square-QAM Signals:

Due to space limitations, we will present in this paper the main derivation steps without delving too much into details. For detailed proofs of the disclosed results, the reader is referred to the complete journal version of this work in [23]. Since the coded bits are assumed to be statistically independent (due to the large-size interleaver), the transmitted symbols (which are simply some *soft* representations for different blocks of these bits) are also independent thereby leading to:

$$p[\boldsymbol{y};\boldsymbol{\alpha}] = \prod_{k=k_0}^{k_0+K-1} p[y(k);\boldsymbol{\alpha}]. \tag{19}$$

Consequently, the global LLF breaks down to the sum of the elementary LLFs (pertaining to each received sample), i.e., $L(\boldsymbol{y};\boldsymbol{\alpha}) = \sum_{k=k_0}^{k_0+K-1} \ln\big(p[y(k);\boldsymbol{\alpha}]\big)$. In this section, we will show for any square-QAM constellation that the pdf of each received sample, $p[y(k);\boldsymbol{\alpha}]$, is further factorized into the product of two analogous terms linearizing thereby the elementary LLFs. Then, owing to the apparent symmetries between the two analogous terms, it is possible to derive the analytical expressions for the considered bounds in section V.

To start with, it can be seen from (1) that:

$$\begin{aligned} p\big[y(k);\boldsymbol{\alpha}\big] &= \sum_{c_m \in \mathcal{C}_p} Pr\big[x(k)=c_m\big]\ p\big[y(k);\boldsymbol{\alpha}|x(k)=c_m\big], \\ &= \sum_{c_m \in \mathcal{C}_p} \frac{Pr\big[x(k)=c_m\big]}{2\pi\sigma^2} \exp\left\{\frac{|y(k)-S_{\phi,\nu}\ c_m|^2}{2\sigma^2}\right\}, \end{aligned} \tag{20}$$

in which we use the shorthand notation $S_{\phi,\nu} \triangleq Se^{j(2\pi k\nu+\phi)}$. Moreover, denoting $I(k) \triangleq \Re\{y(k)\}$ and $Q(k) \triangleq \Im\{y(k)\}$, it can be shown that:

$$p[y(k);\boldsymbol{\alpha}] = \frac{1}{2\pi\sigma^2} e^{-\frac{I(k)^2+Q(k)^2}{2\sigma^2}} D_{\boldsymbol{\alpha}}(k), \tag{21}$$

where the term $D_{\boldsymbol{\alpha}}(k)$ is defined as:

$$D_{\boldsymbol{\alpha}}(k) \triangleq \sum_{c_m \in \mathcal{C}_p} Pr[x(k)=c_m] e^{-\rho|\tilde{c}_m|^2} \exp\left\{\frac{\Re\{c_m y(k)^* S_{\phi,\nu}\}}{\sigma^2}\right\}.$$

In the sequel, we will further manipulate $D_{\boldsymbol{\alpha}}(k)$ by exploiting other hidden properties of the Gray-coding mechanism which are demystified through our recursive construction process introduced in section III (see Fig. 1). Actually, by focusing on square QAM-modulated constellations (i.e., $M=2^{2p}$ for any $p \geq 1$), it can be seen that their alphabet is expressed in the I/Q plane as $\mathcal{C}_p = \big\{\pm(2i-1)d_p \pm j(2n-1)d_p\big\}_{i,n=1,2,...,2^{p-1}}$, where $2d_p$ is the intersymbol distance. For normalized-energy square

$$D_{\boldsymbol{\alpha}}(k)=\sum_{\tilde{c}_m\in\tilde{\mathcal{C}}_p} e^{-\rho|\tilde{c}_m|^2}\Bigg(Pr[x(k)=\tilde{c}_m]\exp\left\{\frac{\Re\left\{\tilde{c}_m y^*(k)S_{\phi,\nu}\right\}}{\sigma^2}\right\}+Pr[x(k)=-\tilde{c}_m]\exp\left\{\frac{\Re\left\{-\tilde{c}_m y^*(k)S_{\phi,\nu}\right\}}{\sigma^2}\right\}$$
$$+Pr[x(k)=\tilde{c}_m^*]\exp\left\{\frac{\Re\left\{\tilde{c}_m^* y^*(k)S_{\phi,\nu}\right\}}{\sigma^2}\right\}+Pr[x(k)=-\tilde{c}_m^*]\exp\left\{\frac{\Re\left\{-\tilde{c}_m^* y^*(k)S_{\phi,\nu}\right\}}{\sigma^2}\right\}\Bigg). \quad (22)$$

QAM constellations $\left(\text{i.e., } \frac{1}{2^{2p}}\sum_{m=1}^{2^{2p}}|c_m|^2=1\right)$, it can be shown (cf. [20]) that $d_p=2^{p/2-1}\left[\sum_{m=1}^{2^{p-1}}(2m-1)^2\right]^{-1/2}$. Now, using $\mathcal{C}_p=\tilde{\mathcal{C}}_p\cup(-\tilde{\mathcal{C}}_p)\cup\tilde{\mathcal{C}}_p^*\cup(-\tilde{\mathcal{C}}_p^*)$ and the fact that $\tilde{c}_m$, $\tilde{c}_m^*$, $-\tilde{c}_m$, and $-\tilde{c}_m^*$ have the same modulus, we rewrite $D_{\boldsymbol{\alpha}}(k)$ in the equivalent form given by (22) shown on the top of the next page. Then, after replacing the *a priori* probabilities involved in (22) by their explicit expressions established in (15) to (18) and recurring to the identity $e^x+e^{-x}=2\cosh(x)$, it can be shown that:

$$D_{\boldsymbol{\alpha}}(k)\;=\;2\beta_k\sum_{\tilde{c}_m\in\tilde{\mathcal{C}}_p}\mu_{k,p}(\tilde{c}_m)\;e^{-\rho|\tilde{c}_m|^2}\times$$
$$\left[\cosh\left(\frac{\Re\left\{\tilde{c}_m\;y^*(k)S_{\phi,\nu}\right\}}{\sigma^2}+\frac{L_{2p-1}(k)}{2}+\frac{L_{2p}(k)}{2}\right)\right.$$
$$\left.+\cosh\left(\frac{\Re\left\{\tilde{c}_m^*\;y^*(k)S_{\phi,\nu}\right\}}{\sigma^2}+\frac{L_{2p-1}(k)}{2}-\frac{L_{2p}(k)}{2}\right)\right]. \quad (23)$$

Furthermore, by using the relationship $\cosh(x)+\cosh(y)=2\cosh(\frac{x+y}{2})\cosh(\frac{x-y}{2})$ along with the two identities $\tilde{c}_m+\tilde{c}_m^*=2\Re\{\tilde{c}_m\}$ and $\tilde{c}_m-\tilde{c}_m^*=2j\Im\{\tilde{c}_m\}$, it follows that:

$$D_{\boldsymbol{\alpha}}(k)=4\beta_k\sum_{\tilde{c}_m\in\tilde{\mathcal{C}}_p}\mu_{k,p}(\tilde{c}_m)e^{-\rho|\tilde{c}_m|^2}\cosh\left(\frac{S\;\Re\{\tilde{c}_m\}u(k)}{\sigma^2}+\frac{L_{2p}(k)}{2}\right)$$
$$\times\cosh\left(\frac{S\;\Im\{\tilde{c}_m\}\;v(k)}{\sigma^2}-\frac{L_{2p-1}(k)}{2}\right), \quad (24)$$

where

$$u(k)\triangleq\Re\left\{y^*(k)e^{j(\phi+2\pi k\nu)}\right\}\text{ and }v(k)\triangleq\Im\left\{y^*(k)e^{j(\phi+2\pi k\nu)}\right\}.$$

Using the fact that $\tilde{\mathcal{C}}_p=\left\{(2i-1)d_p+j(2n-1)d_p\right\}_{i,n=1}^{2^{p-1}}$, one can replace the single sum over $\tilde{c}_m\in\tilde{\mathcal{C}}_p$ in (24) by a double sum over the two counters i and n after replacing $\tilde{c}_m$ by $(2i-1)d_p+j(2n-1)d_p$. Therefore, if we are able to factorize $\mu_{k,p}(\tilde{c}_m)$ as the product of two terms, one depending on i only and the other on n only, then $D_{\boldsymbol{\alpha}}(k)$ will be factorized as well by splitting the two sums (over i and n). To do so, notice from (12) that the two LSBs, $\bar{b}_{2p-1}^m$ and $\bar{b}_{2p}^m$, are not involved in the expression of $\mu_{k,p}(\tilde{c}_m)$ and thus they will be simply denoted as $\times\times$. In addition, we will refer to the first $2p-4$ MSBs by $\bar{\boldsymbol{b}}_p^m$, i.e., $\bar{\boldsymbol{b}}_p^m\triangleq\bar{b}_1^m\bar{b}_2^m\cdots\bar{b}_l^m\cdots\bar{b}_{2p-5}^m\bar{b}_{2p-4}^m$. For more mathematical convenience that will become apparent shortly, we will rather use the superscript (i,n) instead of m in the left-hand side of (6) since $\tilde{c}_m=(2i-1)d_p+j(2n-1)d_p$, i.e.:

$$\tilde{c}_m\longleftrightarrow\bar{\boldsymbol{b}}_p^{(i,n)}\bar{b}_{2p-3}^{(i,n)}\bar{b}_{2p-2}^{(i,n)}\times\times. \quad (25)$$

Now, each point $\tilde{c}_m$ in $\tilde{\mathcal{C}}_p$ with coordinates $\left([2i-1]d_p\,,[2n-1]d_p\right)$ in the Cartesian coordinate system (CCS) of the underlying 2^{2p}-QAM is obtained from (coincides exactly with) a point $c_{m'}$ in the previous $2^{2(p-1)}$-QAM. This is because the latter is placed as is in $\tilde{\mathcal{C}}_p$ (during "step 1"). Furthermore, $c_{m'}$ has its own coordinates, $\left([2i'-1]d_p\,,[2n'-1]d_p\right)$, in the CCS associated to the $2^{2(p-1)}$-QAM constellation. It can be shown that $c_{m'}$ can be expressed in terms of (i,n) as follows:

$$c_{m'}\;=\;(2i-1-2^{p-1})d_p\;+\;j(2n-1-2^{p-1})d_p. \quad (26)$$

Equivalently, denoting the top-right quadrant of the $2^{2(p-1)}$-QAM constellation by $\tilde{\mathcal{C}}_{p-1}$, the symbol $c_{m'}$ itself belongs to its own set of four symmetrical points, i.e., $c_{m'}\in\{\tilde{c}_{m'},-\tilde{c}_{m'},\tilde{c}_{m'}^*,-\tilde{c}_{m'}^*\}$ for some $\tilde{c}_{m'}\in\tilde{\mathcal{C}}_{p-1}$. Recall also that the $2^{2(p-1)}$-QAM constellation itself is obtained from another (lower-order) $2^{2(p-2)}$-QAM Gray-coded constellation, by applying the same recursive process. Then, owing to the three symmetries of "*step 2*", it follows that $\tilde{c}_{m'}$, $-\tilde{c}_{m'}$, $\tilde{c}_{m'}^*$, and $-\tilde{c}_{m'}^*$ [which represent $2(p-1)$ bits each] have the same $2(p-1)-2=2p-4$ MSBs. These common MSBs form excatly the bit sequence encapsulated by $\bar{\boldsymbol{b}}_p^{(m)}$ (that corresponds to c_m). By definition, they are also the only bits involved in the expression of $\mu_{k,p-1}(\tilde{c}_{m'})$, i.e., $\mu_{k,p-1}(\tilde{c}_{m'})=\prod_{l=1}^{2(p-1)-2}e^{(2\bar{b}_l^m-1)\frac{L_l(k)}{2}}$. Using the latter result in (12), we obtain the following recursive property:

$$\mu_{k,p}(\tilde{c}_m)=\mu_{k,p-1}(\tilde{c}_{m'})\exp\left\{(2\bar{b}_{2p-3}^{(i,n)}-1)L_{2p-3}(k)/2\right\}\times$$
$$\exp\left\{(2\bar{b}_{2p-2}^{(i,n)}-1)L_{2p-2}(k)/2\right\}. \quad (27)$$

Now, using $\lfloor x\rfloor$ to denote the floor function, we obtain the following result for the two remaining bits involved in (27):

Lemma 1: $\forall\;i,n=1,2,\cdots,2^{p-1}$, the two bits $\bar{b}_{2p-3}^{(i,n)}$ and $\bar{b}_{2p-2}^{(i,n)}$ are expressed as:

$$\bar{b}_{2p-2}^{(i,n)}=\left\lfloor\frac{i-1}{2^{p-2}}\right\rfloor\qquad\text{and}\qquad\bar{b}_{2p-3}^{(i,n)}=\left\lfloor\frac{n-1}{2^{p-2}}\right\rfloor. \quad (28)$$

Proof: see Appendix A of [23].

By revisiting (27) and considering the recursive construction of $\tilde{\mathcal{C}}_{p-1}$ from the $2^{2(p-2)}$-QAM constellation and following the same reasoning from (25) through (27), one can express $\mu_{k,p-1}(\tilde{c}_{m'})$ itself in the same recursive form of (27). We capitalize on this observation along with the result in (26) to show, by mathematical induction, the following decomposition (cf. [23]):

$$\mu_{k,p}(\tilde{c}_m)=\theta_{k,2p}(i)\theta_{k,2p-1}(n),\;\forall\;p\geq2 \quad (29)$$

where $\theta_{k,2p}(i)$ and $\theta_{k,2p-1}(n)$ are computed recursively, from lower-order constellations, for any $p\geq2$ as follows:

$$\theta_{k,2p}(i)\;=\;\theta_{k,2p-2}\left(\frac{|2i-1-2^{p-1}|+1}{2}\right)\times$$
$$\exp\left\{\left(2\lfloor\frac{i-1}{2^{p-2}}\rfloor-1\right)\frac{L_{2p-2}(k)}{2}\right\}, \quad (30)$$

$$\theta_{k,2p-1}(n)\;=\;\theta_{k,2p-3}\left(\frac{|2n-1-2^{p-1}|+1}{2}\right)\times$$
$$\exp\left\{\left(2\lfloor\frac{n-1}{2^{p-2}}\rfloor-1\right)\frac{L_{2p-3}(k)}{2}\right\}, \quad (31)$$

with $\theta_{k,2}(1)=\theta_{k,1}(1)=1$ since we have extended the definition of $\mu_{k,p}(.)$ for $p=1$ (i.e., QPSK constellations) to be $\mu_{k,1}(c_m)=1\;\forall\;c_m\in\mathcal{C}_1$ [just after eq. 14)]. Plugging (29) in (24) and using the

$$D_{\boldsymbol{\alpha}}(k) = 4\beta_k \sum_{i=1}^{2^{p-1}} \sum_{n=1}^{2^{p-1}} \Big[\theta_{k,2p}(i) e^{-\rho d_p^2 (2i-1)^2} \cosh\Big(\tfrac{S(2i-1)d_p u(k)}{\sigma^2} + \tfrac{L_{2p}(k)}{2}\Big) \times \theta_{k,2p-1}(n) e^{-\rho d_p^2 (2n-1)^2} \cosh\Big(\frac{S(2n-1)d_p v(k)}{\sigma^2} - \frac{L_{2p-1}(k)}{2}\Big)\Big]. \quad (32)$$

trivial identities $|\tilde{c}_m|^2 = d_p^2\big([2i-1]^2 + [2n-1]^2\big)$ and $\tilde{\mathcal{C}}_p = \{(2i-1)d_p + j(2n-1)d_p\}_{i,n=1,2,\cdots,2^{p-1}}$, the term $D_{\boldsymbol{\alpha}}(k)$ is rewritten as in (32) shown on the top of the next page. Finally, after splitting the two sums in (32), $D_{\boldsymbol{\alpha}}(k)$ is factorized as follows:

$$D_{\boldsymbol{\alpha}}(k) = 4\beta_k F_{2p,\boldsymbol{\alpha}}\big(u(k)\big) \times F_{2p-1,\boldsymbol{\alpha}}\big(v(k)\big), \quad (33)$$

where the function $F_{q,\boldsymbol{\alpha}}(.)$ is given by:

$$F_{q,\boldsymbol{\alpha}}(x) = \sum_{i=1}^{2^{p-1}} \theta_{k,q}(i) e^{-\rho d_p^2 (2i-1)^2} \times \cosh\left(\frac{(2i-1)d_p S x}{\sigma^2} + \frac{(-1)^q L_q(k)}{2}\right), \quad (34)$$

and q is a generic counter that is used, from now on, to refer to $2p$ or $2p-1$ depending on the context. Now, using (33) in (21) and then the obtained result in (19), the LLF is obtained as follows:

$$L_{\boldsymbol{y}}(\boldsymbol{\alpha}) = -K\ln(2\pi\sigma^2) - \frac{1}{2\sigma^2}\sum_{k=0}^{K-1}\Big(I(k)^2 + Q(k)^2\Big) + \sum_{k=0}^{K-1}\ln\big(F_{2p,\boldsymbol{\alpha}}(u(k))\big) + \sum_{k=0}^{K-1}\ln\big(F_{2p-1,\boldsymbol{\alpha}}(v(k))\big), \quad (35)$$

involving thereby the sum of two analogous terms (the two last sums). Further, injecting (33) in (21) and using the fact that $I(k)^2 + Q(k)^2 = u(k)^2 + v(k)^2$, it can be shown that $p[y(k);\boldsymbol{\alpha}]$ factorizes as follows:

$$p[y(k);\boldsymbol{\alpha}] = p[u(k), v(k);\boldsymbol{\alpha}] = p[u(k);\boldsymbol{\alpha}]p[v(k);\boldsymbol{\alpha}], \quad (36)$$

where

$$p[u(k);\boldsymbol{\alpha}] = \frac{2\beta_{k,2p}}{\sqrt{2\pi\sigma^2}} e^{-\frac{u(k)^2}{2\sigma^2}} F_{2p,\boldsymbol{\alpha}}(u(k)), \quad (37)$$

$$p[v(k);\boldsymbol{\alpha}] = \frac{2\beta_{k,2p-1}}{\sqrt{2\pi\sigma^2}} e^{-\frac{v(k)^2}{2\sigma^2}} F_{2p-1,\boldsymbol{\alpha}}(v(k)), \quad (38)$$

with

$$\beta_{k,2p} = \prod_{l=1}^{p} \frac{1}{2\cosh\big(\frac{L_{2l}(k)}{2}\big)}, \quad \beta_{k,2p-1} = \prod_{l=2}^{p} \frac{1}{2\cosh\big(\frac{L_{2l-1}(k)}{2}\big)}.$$

The pdfs established in (37) and (38) will be used to derive the different FIM elements in the next section.

V. Derivation of the CA CRLBs

Due to space limitations, we will provide here the derivation details only for the first FIM element since the other ones can be obtained in the same way. Starting from (35), we readily have the following result:

$$\mathrm{E}\left\{\frac{\partial^2 \ln(p[\boldsymbol{y};\boldsymbol{\alpha}])}{\partial S^2}\right\} = \sum_{k=0}^{K-1}\mathrm{E}\left\{\frac{\partial^2 \ln(F_{2p,\boldsymbol{\alpha}}(u(k)))}{\partial S^2}\right\} + \sum_{k=0}^{K-1}\mathrm{E}\left\{\frac{\partial^2 \ln(F_{2p-1,\boldsymbol{\alpha}}(v(k)))}{\partial S^2}\right\}. \quad (39)$$

As mentioned previously, the two terms in the right-hand side of (39) are analogous and they can be derived in the same way, especially because the random variables $u(k)$ and $v(k)$ are *almost* identically distributed. Thus, for ease of notations, we will henceforth use $z_q(k)$ to refer to $u(k)$ when $q = 2p$ and to $v(k)$ when $q = 2p-1$, respectively. Using this generic notation and defining:

$$\dot{F}_{q,\boldsymbol{\alpha}}(z_q(k)) \triangleq \frac{\partial F_{q,\boldsymbol{\alpha}}(z_q(k))}{\partial S}, \quad \ddot{F}_{q,\boldsymbol{\alpha}}(z_q(k)) \triangleq \frac{\partial^2 F_{q,\boldsymbol{\alpha}}(z_q(k))}{\partial S^2},$$

it can be shown that:

$$\mathrm{E}\left\{\frac{\partial^2 \ln(F_{q,\boldsymbol{\alpha}}(z_q(k)))}{\partial S^2}\right\} = \mathrm{E}\left\{\frac{\ddot{F}_{q,\boldsymbol{\alpha}}(z_q(k))}{F_{q,\boldsymbol{\alpha}}(z_q(k))}\right\} - \mathrm{E}\left\{\frac{\dot{F}_{q,\boldsymbol{\alpha}}(z_q(k))^2}{F_{q,\boldsymbol{\alpha}}(z_q(k))^2}\right\}.$$

These two expectations are obtained by integration over the distribution of $z_q(k)$ obtained earlier in (37) and (38) for $q = 2p$ and $q = 2p-1$, respectively. In particular, we have:

$$\mathrm{E}\left\{\frac{\dot{F}_{q,\boldsymbol{\alpha}}(z_q(k))^2}{F_{q,\boldsymbol{\alpha}}(z_q(k))^2}\right\} = \int_{-\infty}^{+\infty} \frac{\dot{F}_{q,\boldsymbol{\alpha}}(z_q(k))^2}{F_{q,\boldsymbol{\alpha}}(z_q(k))^2} p[z_q(k),\boldsymbol{\alpha}] dz_q(k) \quad (40)$$

$$= \frac{2\beta_{k,q}}{\sqrt{2\pi\sigma^2}} \int_{-\infty}^{+\infty} \frac{\dot{F}_{q,\boldsymbol{\alpha}}(z_q(k))^2}{F_{\boldsymbol{\alpha}}(z_q(n))} e^{-\frac{z_q(n)^2}{2\sigma^2}} dz_q(n),$$

where the expression of the first derivative, $\dot{F}_{q,\boldsymbol{\alpha}}(z_q(k))$, is given by:

$$\dot{F}_{q,\boldsymbol{\alpha}}(z_q(k)) = \sum_{i=1}^{2^{p-1}} \theta_{k,q}(i) e^{-\frac{(2i-1)^2 d_p^2 S^2}{2\sigma^2}} \times \left[\frac{(2i-1)d_p z_q(k)}{\sigma^2}\sinh\Big(\frac{(2i-1)d_p S z_q(k)}{\sigma^2} + \frac{L_q(k)}{2}\Big) - \frac{(2i-1)^2 d_p^2 S}{\sigma^2}\cosh\Big(\frac{(2i-1)d_p S z_q(k)}{\sigma^2} + \frac{L_q(k)}{2}\Big)\right]. \quad (41)$$

We further simplify (40) by changing $z_q(k)/\sigma$ by t and using $\rho = S^2/2\sigma^2$ to obtain:

$$\mathrm{E}\left\{\frac{\dot{F}_{q,\boldsymbol{\alpha}}(z_q(k))^2}{F_{q,\boldsymbol{\alpha}}(z_q(k))^2}\right\} = \frac{2\beta_{k,q} d_p^2}{\sigma^2}\psi_{k,q}(\rho), \quad (42)$$

in which $\Psi_{k,q}(\rho)$ is defined as:

$$\Psi_{k,q}(\rho) \triangleq \frac{1}{\sqrt{2\pi}} \int_{-\infty}^{+\infty} \frac{\lambda_{k,q}(\rho,t)^2}{\delta_{k,q}(\rho,t)} \; e^{-\frac{t^2}{2}} dt, \quad (43)$$

where, by using $\omega_{k,q}(i) \triangleq \theta_{k,q}(i)\; e^{-(2i-1)^2 d_p^2 \rho}$, the functions $\delta_{k,q}(.,.)$ and $\lambda_{k,q}(.,.)$ are, respectively, given by (44) and (45) (the latter is shown on the top of the next page):

$$\delta_{k,q}(\rho,t) = \sum_{i=1}^{2^{p-1}} \omega_{k,q}(i)\cosh\Big(\sqrt{2\rho}(2i-1)d_p t + \frac{(-1)^q L_q(k)}{2}\Big). \quad (44)$$

Furthermore, after some algebraic manipulations, we obtain:

$$\mathrm{E}\left\{\frac{\ddot{F}_{q,\boldsymbol{\alpha}}(z_q(k))}{F_{q,\boldsymbol{\alpha}}(z_q(k))}\right\} = \frac{2\beta_{k,q}}{\sqrt{2\pi\sigma^2}} \int_{-\infty}^{+\infty} \ddot{F}_{q,\boldsymbol{\alpha}}(z_q(k)) e^{-\frac{z_q(n)^2}{2\sigma^2}} dz_q(n) = 0.$$

$$\lambda_{k,q}(\rho,t)=\sum_{i=1}^{2^{p-1}}(2i-1)^2\omega_{k,q}(i)\left[t\sinh\left(\sqrt{2\rho}\ (2i-1)d_pt+\frac{(-1)^qL_q(k)}{2}\right)-d_p(2i-1)\sqrt{2\rho}\cosh\left(\sqrt{2\rho}(2i-1)d_pt+\frac{(-1)^qL_q(k)}{2}\right)\right]. \quad (45)$$

Therefore, by using $\alpha_{k,q}\triangleq 2\beta_{k,q}d_p^2\psi_{k,q}(\rho)$ and injecting (42) for $q=2p$ and $q=2p-1$ in (39), it follows that:

$$\mathrm{E}\left\{\frac{\partial^2\ln(P[\boldsymbol{y};\boldsymbol{\alpha}])}{\partial S^2}\right\}=-\frac{1}{\sigma^2}\sum_{k=0}^{K-1}\Big[\alpha_{k,2p}+\alpha_{k,2p-1}\Big]. \quad (46)$$

Equivalent algebraic manipulations, which are omitted due to lack of space, lead to the following analytical expressions for the second FIM's diagonal element:

$$\mathrm{E}\left\{\frac{\partial^2\ln(P(\boldsymbol{y};\boldsymbol{\alpha}))}{\partial{\sigma^2}^2}\right\}=\frac{K}{\sigma^4}+\frac{1}{\sigma^4}\sum_{k=0}^{K-1}\Big[\nu_{k,2p}+\nu_{k,2p-1}\Big], \quad (47)$$

where $\nu_{k,q}$ (for $q=2p$ or $2p-1$) is given by:

$$\nu_{k,q}=c_{4,q}^{(k)}\rho^2+2\left(c_{2,q}^{(k)}-2\beta_{k,q}d_p^2\Phi_{q,k}(\rho)\right)-c_{0,q}^{(k)}. \quad (48)$$

The coefficients $c_{l,q}^{(k)}$ are given by:

$$c_{l,q}^{(k)}=2\beta_{k,q}d_p^l\cosh\left(L_q(k)/2\right)\textstyle\sum_{i=1}^{2^{p-1}}\theta_{k,q}(i)(2i-1)^l, \quad (49)$$

and the function $\Phi_{k,q}(.)$ is defined as:

$$\Phi_{k,q}(\rho)\triangleq\frac{1}{\sqrt{2\pi}}\int_{-\infty}^{+\infty}\frac{\gamma_{k,q}^2(\rho,t)}{\delta_{k,q}(\rho,t)}\ e^{-\frac{t^2}{2}}dt, \quad (51)$$

where $\gamma_{k,q}(.,.)$ is defined by (50) in the top of the next page. Equivalent derivations also yield the following expression for the off-diagonal element of $\boldsymbol{I}(\boldsymbol{\alpha})$:

$$\mathrm{E}\left\{\frac{\partial^2\ln(P[\boldsymbol{y};\boldsymbol{\alpha}])}{\partial\sigma^2\partial S}\right\}=-\frac{S}{\sigma^4}\sum_{k=0}^{K-1}\Big[\eta_{k,2p}+\eta_{k,2p-1}\Big], \quad (52)$$

in which $\eta_{k,q}\triangleq c_{2,q}^{(k)}-2d_p^2\ \beta_{k,q}\ \Omega_{k,q}(\rho)$ with the function $\Omega_{k,q}(.)$ being defined as:

$$\Omega_{k,q}(\rho)\triangleq\frac{1}{\sqrt{2\pi}}\int_{-\infty}^{+\infty}\frac{\gamma_{q,\rho}(t)\lambda_{q,\rho}(t)}{\delta_{q,\rho}(t)}\ e^{-\frac{t^2}{2}}dt. \quad (53)$$

Therefore, from (46), (47) and (52), the global FIM decomposes into the sum of K elementary FIMs:

$$\boldsymbol{I}(\boldsymbol{\alpha})=\textstyle\sum_{k=0}^{K-1}\boldsymbol{I}_k(\boldsymbol{\alpha}) \quad (54)$$

where $\{\boldsymbol{I}_k(\boldsymbol{\alpha})\}_{k=0}^{K-1}$ is the FIM pertaining to the estimation of the SNR from the received sample $y(k)$ alone:

$$\boldsymbol{I}_k(\boldsymbol{\alpha})=\frac{1}{\sigma^4}\begin{pmatrix}\sigma^2\big[\alpha_{k,2p}+\alpha_{k,2p-1}\big] & S\big[\eta_{k,2p}+\eta_{k,2p-1}\big]\\ S[\eta_{k,2p}+\eta_{k,2p-1}] & -\big[\nu_{2p,k}+\nu_{2p-1,k}+1\big]\end{pmatrix}. \quad (55)$$

Now, since the inverse of any (2×2) matrix is directly obtained by swapping the two diagonal elements and negating the off-diagonal ones, it can be shown from (54) that:

$$\boldsymbol{I}^{-1}(\boldsymbol{\alpha})=\textstyle\sum_{k=0}^{K-1}\dfrac{\det\{\boldsymbol{I}_k(\boldsymbol{\alpha})\}}{\det\{\boldsymbol{I}(\boldsymbol{\alpha})\}}\boldsymbol{I}_k^{-1}(\boldsymbol{\alpha}), \quad (56)$$

where $\det\{.\}$ returns the determinant of any square matrix. Finally, using (56) in (4), it can be shown that:

$$\mathrm{CRLB}(\rho)=\textstyle\sum_{k=0}^{K-1}\omega(k)\ \mathrm{CRLB}_k(\rho), \quad (57)$$

where $\omega(k)\triangleq\det\{\boldsymbol{I}_k(\boldsymbol{\alpha})\}/\det\{\boldsymbol{I}(\boldsymbol{\alpha})\}$ and $\mathrm{CRLB}_k(\rho)$, given by (58) on the top of the next page, is the elementary CRLB pertaining to the estimation of the SNR given the received sample $y(k)$ only. Finally, in order to evaluate the different CRLBs derived in this paper, the LLRs of the bits must be computed. Fortunately, owing to the turbo principle, it was shown in [25] that the *extrinsic* information of the bits, which is delivered during the decoding process, is an accurate estimate of these LLRs.

VI. Simulation Results

In this section, we provide graphical representations of the newly derived SNR CRLBs for different modulation orders and different coding rates using $K=207$ received samples. The encoder is composed of two identical RSCs each with systematic rate $R_0=1/2$ and generator polynomials (1,0,1,1) and (1,1,0,1). The size of the RSC encoders' memory is fixed to 4.

In Figs. 2 and 3, we plot both the analytical and empirical CA CRLBs for 16-QAM and 64-QAM signals, respectively, with two coding rates (i.e., $R_1=0.3285\approx\frac{1}{3}$ and $R_2=0.4892\approx\frac{1}{2}$). First, we clearly see from both figures a perfect fit between the analytical and empirical CRLBs, in all the considered cases, validating thereby our new analytical expressions. Note here that the empirical CA SNR CRLBs were evaluated by following the same approach proposed earlier in [22] in the context of CA phase estimation.

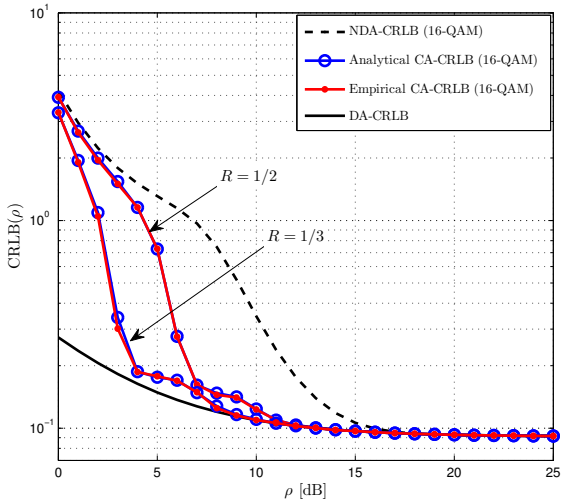

Fig. 2. CA vs. DA and NDA CRLBs for SNR estimation as function of the true SNR ρ with two different rates ($R=1/3,\ 1/2$): 16-QAM.

We see also from both figures that the CRLB for CA estimation is smaller than the CRLB for the NDA scenario. This highlights the potential estimation performance gain that could be achieved by leveraging the information about the transmitted bits that could be gathered during the decoding process. This is in contrast with the traditional NDA scheme where the SNR is estimated directly from the output of the matched filter. Even though the CA scheme performs to the CRLB limit nearly as well as the NDA scheme at low SNR, near 0 dB, it always offers a potential gain (over the latter) that sharply increases with the SNR increasing. For instance, by the SNR value, $\rho=4$ dB, the CA CRLB for 16-QAM signals soon becomes almost 10 times smaller than the NDA CRLB. From this relatively small SNR threshold, the CA CRLB

$$\gamma_{k,q}(\rho,t)=\sum_{i=1}^{2^{p-1}}(2i-1)^2\omega_{k,q}(i)\left[t\sinh\left(\sqrt{2\rho}\ (2i-1)d_p t+\frac{(-1)^q L_q(k)}{2}\right)-d_p(2i-1)\sqrt{\frac{\rho}{2}}\cosh\left(\sqrt{2\rho}(2i-1)d_p t+\frac{(-1)^q L_q(k)}{2}\right)\right]. \quad (50)$$

$$\mathrm{CRLB}_k(\rho)=\frac{100}{\ln(10)^2\rho}\frac{2\left[\nu_{2p,k}(\rho)+\nu_{2p-1,k}(\rho)+1\right]-\left[4\eta_{2p,k}(\rho)+4\eta_{2p-1,k}(\rho)+\alpha_{2p,k}(\rho)+\alpha_{2p-1,k}(\rho)\right]\rho}{\left[\nu_{2p,k}(\rho)+\nu_{2p-1,k}(\rho)+1\right]\left[\alpha_{2p,k}(\rho)+\alpha_{2p-1,k}(\rho)\right]-2\left[\eta_{2p,k}(\rho)+\eta_{2p-1,k}(\rho)\right]\rho}. \quad (58)$$

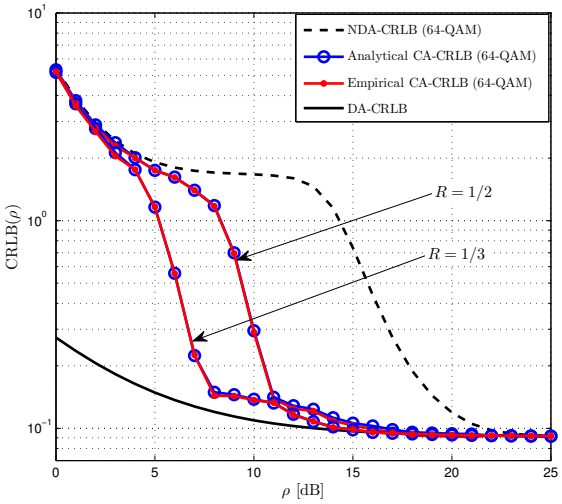

Fig. 3. CA vs. DA and NDA CRLBs for SNR estimation as function of the true SNR ρ with two different rates ($R=1/3,\ 1/2$): 64-QAM.

starts to reach the DA CRLB derived earlier in [19]. Therefore, over a wide range of practical SNRs and without relying on any pilot sequence, CA estimation could potentially turn out to be equivalent to DA estimation which relies on the perfect knowledge of all the bits (or equivalently the symbols).

Figs. 2 and 3 also show clearly the effect of the coding rate, R, on the SNR estimation performance. Even though the CA CRLBs corresponding to the two considered rates ultimately coincide at moderate SNR levels, they exhibit a significant gap at lower SNR values. In fact, with smaller coding rates, more redundancy can potentially be provided by the turbo encoder and the bits could then be decoded more accurately. In this case, the *extrinsic* information, which is used to approximate the LLRs [25, 26], becomes increasingly high (in absolute value) and CA estimation becomes even closer in CRLB performance to DA estimation.

VII. Conclusion

In this contribution, we established the analytical expressions for the CRLBs of SNR estimation from turbo-coded square-QAM transmissions. We have also verified for the sake of validation that our new analytical bounds perfectly match their empirical counterparts obtained here through extensive Monte-Carlo simulations. The new CA CRLBs are smaller than the NDA CRLBs thereby suggesting better SNR estimation potential when properly exploiting the SISO information about the transmitted bits that could be obtained from the decoder. The new CA CRLBs also start to coincide with the DA CRLBs from relatively small SNR thresholds which relatively decrease with lower modulation orders and higher coding rates.

References

[1] S. Talakoub and B. Shahrrava, "Turbo equalization with integrated SNR estimation," in *Proc. IEEE GLOBECOM*, San Francisco, CA, USA, Nov. 27-Dec. 1, 2006.
[2] S. Talakoub and B. Shahrrava, "Turbo equalization with iterative online SNR estimation," in *Proc. IEEE WCNC*, New Orleans, LA, Mar. 13-17, 2005, vol. 2, pp. 1097-1102.
[3] J. G. Proakis, *Digital Communications,* McGraw-Hill, 2001.
[4] K. Balachandran , S. R. Kadaba, and S. Nanda, "Channel quality estimation and rate adaptation for cellular mobile radio,"*IEEE J. Sel. Areas Commun.,* vol. 17, no. 7, pp.1244 -1256, July 1999.
[5] C. Berrou and A. Glavieux, "Near optimum error correcting coding and decoding: turbo codes," *IEEE Trans. Commun.,* vol. 44, no. 10, pp. 1261-1271, Oct. 1996.
[6] E. Dahlman, S. Parkvall, J. Sköld, and P. Beming, *3G Evolution: HSPA and LTE for Mobile Broadband,* Oxford, UK: Academic Press, 2007.
[7] 3GPP TS 36.211: 3rd Generation Partnership Project; Technical Specification Group Radio Access Network; Evolved Universal Terrestrial Radio Access (E-UTRA); Physical Channels and Modulation.
[8] N. Wu, H. Wang, and J. M. Kuang, "Maximum likelihood signal-to-noise ratio estimation for coded linearly modulated signals," *IET Commun.*, vol. 4, pp. 265-271, 2010.
[9] M. Bergmann, W. Gappmair, H. Schlemmer, and O. Koudelka, "Code-aware joint estimation of carrier phase and SNR for linear modulation schemes", in *Proc. 5th Advanced Satellite Multimedia Systems Conference*, Cagliari, Italy, Sept. 13-15, 2010, pp. 177-182.
[10] K. T. Shr and Y. H. Huang, "SNR estimation based on metric normalization frequency in Viterbi decoder," *IEEE Commun. Lett.,* vol. 15, no. 6, pp. 668-670, June 2011.
[11] M. A. Dangl and J. Lindner, "How to use a priori information of data symbols for SNR estimation," *IEEE Signal Process. Lett.*, vol. 13, no. 11, pp. 661-664, Nov. 2006.
[12] S. Minying, L. Yuan, and S. Sumei, "Impact of SNR estimation error on turbo code with high-order modulation," in *Proc. IEEE VTC-Spring,* Milan, Italy, May 17-19, 2004..
[13] M. A. Boujelben, F. Bellili, S. Affes, and A. Stéphenne, "SNR estimation over SIMO channels from linearly-modulated signals," *IEEE Trans. Signal Process.,* vol. 58, no. 12, pp. 6017-6028, Dec. 2010.
[14] M. A. Boujelben, F. Bellili, S. Affes, and A. Stéphenne, "EM algorithm for non-data-aided SNR estimation of linearly-modulated signals over SIMO channels," presented at the IEEE GLOBECOM, Honolulu, HI, USA, Dec. 2009.
[15] A. Stéphenne, F. Bellili, and S. Affes, "Moment-based SNR estimation over linearly-modulated wireless SIMO channels," *IEEE Trans. Wireless Commun.*, vol. 9, no. 2, pp. 714-722, Feb. 2010.
[16] A. Stéphenne, F. Bellili, and S. Affes, "Moment-based SNR estimation for SIMO wireless communication systems using arbitrary QAM," in *Proc. 41st Asilomar Conf. Signals, Syst., Comput.,* Pacific Grove, CA, USA, Nov. 4-7, 2007, pp. 601-605.
[17] F. Bellili, R. Meftehi, S. Affes, and A. Stéphenne "Maximum likelihood SNR estimation over time-varying flat-fading SIMO channels," presented at the IEEE ICASSP, Florence, Italy, May 4-9, 2014.
[18] S. M. Kay, *Fundamentals of Statistical Signal Processing, vol 1: Estimation Theory*, Prentice-Hall, 1993.
[19] N. S. Alagha, "Cramér-Rao bounds of SNR estimates for BPSK and QPSK modulated signals," *IEEE Commun. Lett.,* vol. 5, pp. 10-12, Jan. 2001.
[20] F. Bellili , A. Stéphenne, and S. Affes, "Cramér-Rao lower bounds for NDA SNR estimates of square QAM modulated transmissions," *IEEE Trans. Commun.,* vol. 58, no. 11, pp. 3211-3218, Nov. 2010.
[21] F. Bellili, A. Stéphenne, and S. Affes, "Cramér-Rao bounds for NDA SNR estimates of square QAM modulated signals," presented at the IEEE WCNC, Budapest, Hungary, Apr. 2009.
[22] N. Noels, H. Steendam, and M. Moeneclaey, "The Cramér-Rao bound for phase estimation from coded linearly modulated signals," *IEEE Commun. Lett.,* vol. 7, no. 5, pp. 207-209, May 2003
[23] F. Bellili, A. Methenni, and S. Affes, "Closed-Form CRLBs for SNR estimation from Turbo-coded BPSK-, MSK-, and square-QAM-modulated signals," *IEEE Trans. Signal Process.,* vol. 58, no. 15, pp. 4018-4033, Aug. 2014.
[24] L. Bahl, J. Cocke, F. Jelinek, and J. Raviv, "Optimal decoding of linear codes for minimizing symbol error rate", *IEEE Trans. Inf. Theory*, vol. IT-20(2), no. 2, pp.284-287, Mar. 1974.
[25] G. Colavolpe, G. Ferrari, and R. Raheli, "Extrinsic information in iterative decoding: A unified view," *IEEE Trans. Commun.,* vol. 49, no. 12, pp. 2088-2094, Dec. 2001.
[26] L. Zhang and A. Burr "Iterative carrier phase recovery suited for turbo-coded systems," *IEEE Trans. Wireless Commun.,* vol. 3, no. 6, pp. 2267-2276, Nov. 2004.